COBEM 2023 27TH INTERNATIONAL CONGRESS OF MECHANICAL ENGINEERING

ABCM Brazilian Society of Mechanical Sciences and Engineering
27th ABCM International Congress of Mechanical Engineering
December 04-08, 2023, Florianópolis-SC, Brazil

COB-2023-0515
CFD ANALYSIS OF AN ULTRASONIC FLOWMETER UNDER DIFFERENT FLOW CONDITIONS

Augusto Cheffer
Petróleo Brasileiro S.A. (PETROBRAS)
Engineering, Technology and Innovation
Submarine Engineering
20.231.300 – Rio de Janeiro – RJ – Brazil
augusto.cheffer@poli.ufrj.br

Douglas de Almeida Garcia
Fábio Ouverney Costa
National Institute of Metrology, Quality and Technology (INMETRO)
Fluid Dynamics Metrology Division (DINAM)
25.250.020 – Duque de Caxias – RJ – Brazil
dagarcia@inmetro.gov.br, focosta@inmetro.gov.br

Luiz Octavio Pereira
Petróleo Brasileiro S.A. (PETROBRAS)
Research, Development and Innovation Center (CENPES)
21.941.915 – Rio de Janeiro – RJ – Brazil
luizoctavio@petrobras.com.br

Bruno Almeida
SIMEC Engenharia LTDA
21.940.180 – Rio de Janeiro – RJ – Brazil
bruno@simecengenharia.com.br

Philippe Rollemberg d'Egmont
Universidade Federal do Rio de Janeiro
COPPE – Department of Mechanical Engineering
21.941.972 – Rio de Janeiro – RJ – Brazil
philipperegmont@gmail.com

Abstract. *Some flow measurement technologies are directly influenced by the physical properties of the fluid and flow velocity profile. The use of ultrasonic flowmeters has evolved over the past decades and today is one of the most promising technologies for flow measurement under different process conditions in the oil and natural gas industry. The advantages of ultrasonic flowmeters are specially related to its non-intrusiveness and low pressure drop, combined with low uncertainty and high turn-down ratio. In addition, they are little susceptible to mechanical wear and can be used in bidirectional flow measurements. In short, an ultrasonic flowmeter works as a flow velocity meter and its performance is related to its design (path topology and algorithms of integration) and installation and process conditions (temperature, pressure, wall roughness, flow regime, etc). This work evaluates the theoretical performance of a hypothetical 6 inches, 8-path transit time ultrasonic flowmeter (two 4-path gauss-jacobi distributed crossed planes). Such evaluation is carried out through CFD numerical analysis, using Ansys Workbench® software. A common pipe installation design found in oil and natural gas industry is studied. The analyzed fluids are water and 4 different viscosities oils, with a Reynolds number ranging from 492 to 1.2x10^6. The results show the effects of different installation designs on the velocity field, as well as the formation of secondary flows and generation of vortices. Furthermore, it is also observed that the studied flowmeter design has a great ability to minimize, or even eliminate, rotational effects in the flow. However, the distortion of the velocity profile can still significantly affect its performance.*

Keywords: *ultrasonic flow meter, computational fluid dynamics (CFD), numerical methods, turbulent flow.*

1. INTRODUCTION

Some flow measurement technologies are directly influenced by the rheology and physical properties of the fluid. In this context, (Inmetro/ANP, 2013) establishes the necessity of calibrating flow meters under usual operation conditions, or with similar fluid, admitting some duly specified deviations. This work aims to study the influence of flow conditions on multi-path ultrasonic flow meters, ultimately motivated by modernization of meter technologies based on industrial community experience (AGA, 2017) that point the possibility to use Reynolds number for calibration of ultrasonic meters.

The use of Computational Fluid Dynamics (CFD) as a support tool for research in fluid dynamics becomes of great value due to the costs and time involved in carrying out laboratory tests. Although they cannot replace traceable calibrations, simulations are well-established tools and can guide the design of test matrices and supplement information obtained in experiments, in such a way that new scenarios can be explored - which would be unfeasible to carry out, for reasons practical, logistical or budgetary – leading to greater confidence and scope in the conclusions obtained.

This work deals with CFD simulations, performed in Ansys Workbench® software, to investigate flow conditions that are commonly found in industrial plants and their effects on ultrasonic flow meters performance. The results of this study may technically support changes in regulatory requirements related to the calibration of flow meters, reducing costs and improving the logistical dynamics of these processes for the oil, natural gas, energy and biofuels industry.

2. METHODOLOGY

The methodology used consists of developing the geometry of the piping, generating the mesh, determining the flowrate and fluid properties, choosing the physical model, determining the boundary conditions and describing the sensors. Each step is following described.

2.1 Geometry and fluid properties

To study the effects of curves, a 6" (152.4 mm) diameter pipe with a 90° elbow of 229 mm radius is considered. The sensor is positioned 5 diameters (760 mm) downstream from the elbow as shown in Figure 1. The dimensions adopted are in accordance with the ANSI B 16.9 standard (HHG, 2012).

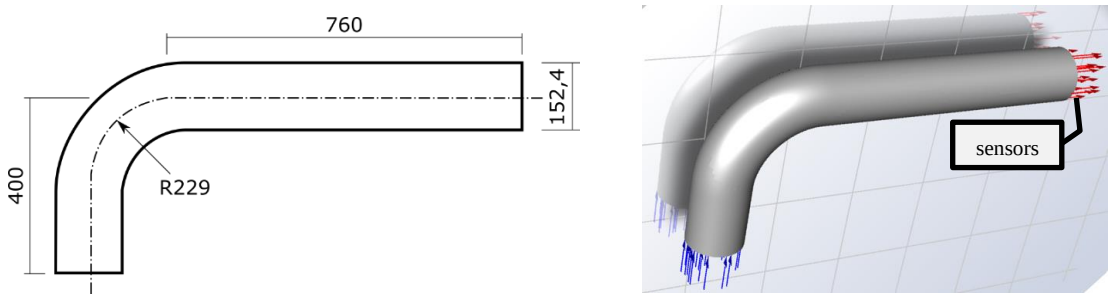

Figure 1. Pipe geometry considered in analysis (units: mm).

In this work five different fluids are considered, whose properties are listed in Table 1. For each fluid, an analysis with different flowrates is performed. Table 2 shows flow rates, mean velocity and Reynolds number for each fluid.

Table 1. Properties of fluids used in simulations.

Fluid	Temperature [°C]	Density [kg/m^3]	Dynamic Viscosity [cP]
Water	20	998.2	1.008
Mineral Oil HR-5-EP	20	845	7.55
Mineral Oil HR-22-EP	20	860	47.12
Mineral Oil HR-32-EP	20	863	68.88
Mineral Oil HR-100-EP	20	880	272.80

Table 2. Flow rates, mean velocity and Reynolds for each fluid used in simulations.

Fluid	Flow rate [m³/h]	Mean Velocity [m/s]	Reynolds number
Water	525.354	8.00	1,207,347
	459.685	7.00	1,056,428
	394.016	6.00	905,510
	262.677	4.00	603,673
	197.008	3.00	452,755
	131.339	2.00	301,837
	65.669	1.00	150,918
	26.268	0.40	60,367
	13.134	0.20	30,184
	6.577	0.10	15,115
HR-5-EP	525.354	8.00	136,376
	459.685	7.00	119,329
	394.016	6.00	102,282
	328.346	5.00	85,235
	262.677	4.00	68,188
	197.008	3.00	51,141
	131.339	2.00	34,094
	65.669	1.00	17,047
	45.969	0.70	11,933
	26.268	0.40	6,819
	13.134	0.20	3,409
	6.567	0.10	1,705
HR-22-EP	525.354	8.00	22,252
	394.016	6.00	16,689
	328.346	5.00	13,908
	262.677	4.00	11,126
	197.008	3.00	8,345
	131.339	2.00	5,563
	65.669	1.00	2,782
	45.969	0.70	1,947
HR-32-EP	525.354	8.00	15,274
	328.346	5.00	9,546
	197.008	3.00	5,728
	65.669	1.00	1,909
HR-100-EP	525.354	8.00	3,933
	394.016	6.00	2,950
	262.677	4.00	1,966
	131.339	2.00	983
	65.669	1.00	492

2.2 Numerical model

The hypotheses are steady and fully developed flow, without thermal exchange, absolute pressure of 1 atm and relative pressure equal to 0 Pa at the outlet. The adopted turbulence model is the k-ω SST, which is based on the mean Navier-Stokes equations (RANS), which combines the advantages of the traditional k-ω model with the k-ε model, allowing better capture of the turbulent phenomena near and far from the pipe walls (ANSYS, 2012). The convergence criterion is set such that the residual between iterations must be smaller than 10^{-4}.

Figure 2 shows the mesh applied. It has 60452 elements and is refined near to pipe wall using a native configuration called inflation, whose parameters are: 5 layers; first layer height of $8.0\text{x}10^{-4}$ m; and growing rate of 1.5. CPU time consumed in each simulation is 8.34 s for a 2th Gen Intel® Core™ i5-1245U processor using 6 cores.

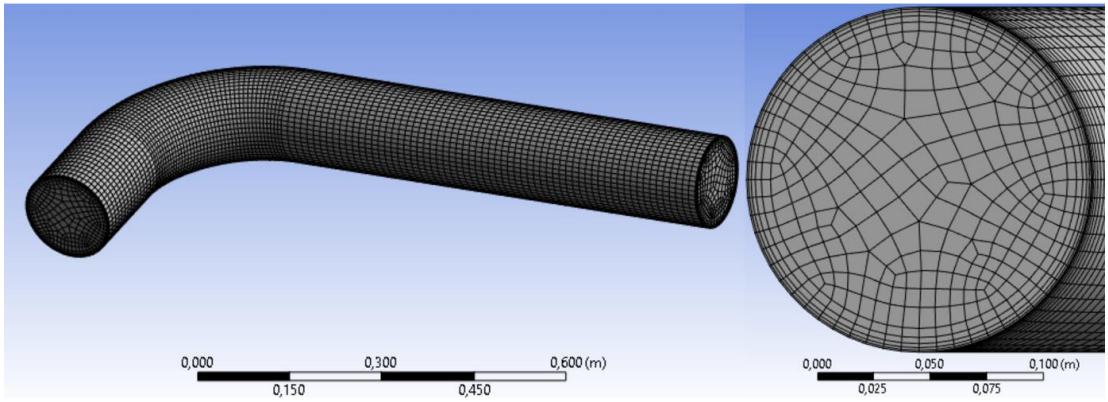

Figure 2. Mesh constructed for ultrasonic meter.

The pipeline is extended so that the fully developed flow condition is satisfied, thus allowing comparison between different cases without interference from boundary layer development effects. The literature (Fox *et al*., 2011) indicates the minimum length to guarantee the developed flow, according to Eqs. (1) and (2):

$$L_e \cong 0{,}06D(Re) \qquad [Laminar] \tag{1}$$

$$L_e \cong 4{,}40D\left(Re^{\frac{1}{6}}\right) \qquad [Turbulent]. \tag{2}$$

Preliminary simulations are conducted in a straight section of pipe, carefully chosen to ensure complete flow development. The exit velocity profiles obtained from these simulations are then utilized as input conditions for the studied geometry.

2.3 Sensors

The analyzed ultrasonic meter configuration has 8 paths (sensors), distributed in two crossed planes with an angle of 60 degrees (as illustrated in Figure 3), which is one of the most common designs in industry. The positioning and weights for each path follow the Gauss-Chebyshev quadrature theory and are presented in Table 3.

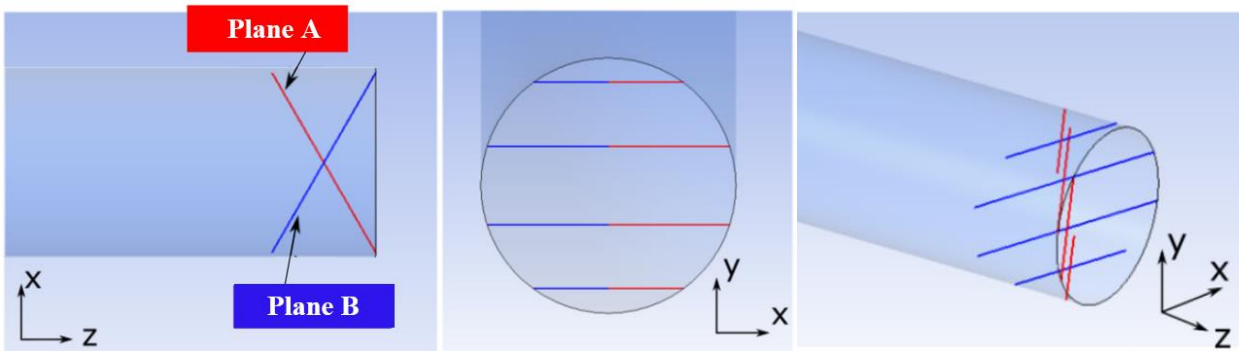

Figure 3. Configuration of ultrasonic meter.

Table 3. Weights and positions for Gauss-Chebyshev quadrature.

Sensor	y-axis position	Weight - ω_i	$\frac{2}{\pi}\omega_i$
1	-0.80902	0.21708	0.13820
2	-0.309017	0.56832	0.36180
3	0.309017	0.56832	0.36180
4	0.80902	0.21708	0.13820

In *Ansys*®, each sensor is represented by a line element, in which the coordinates (X, Y and Z) of the initial and final points must be provided. To determine these points, the coordinates are calculated based on the location of chords and geometric concepts as follows:

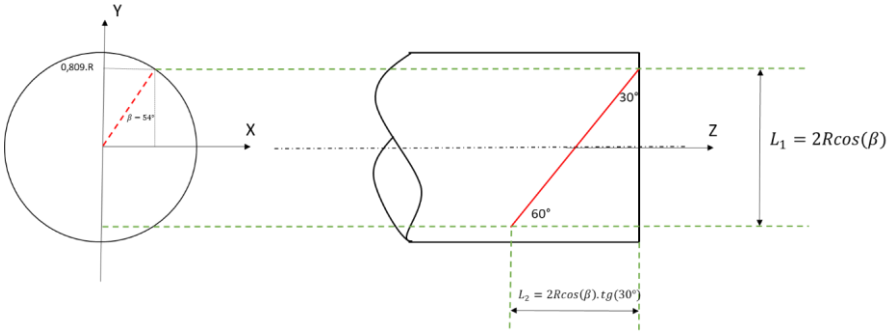

Figure 4. Position of Sensor 1.

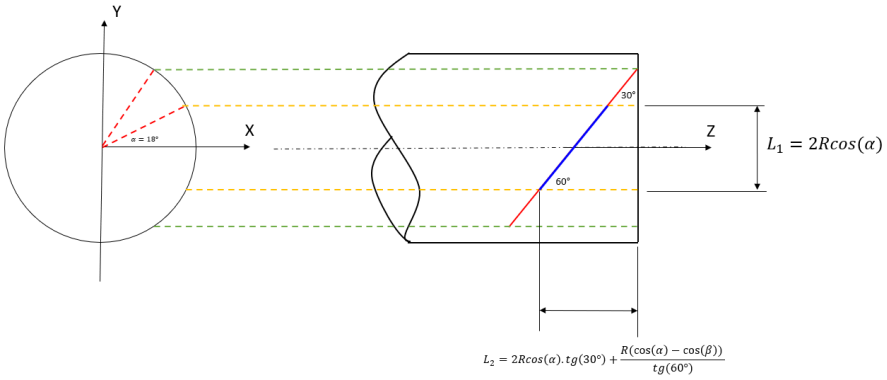

Figure 5. Position of Sensor 2.

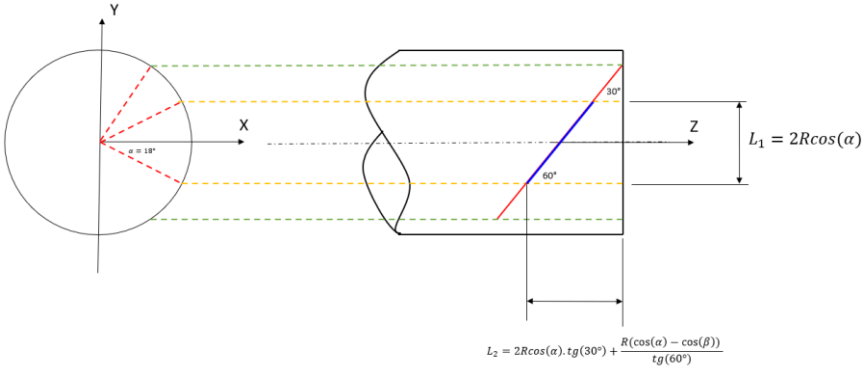

Figure 6. Position of Sensor 3.

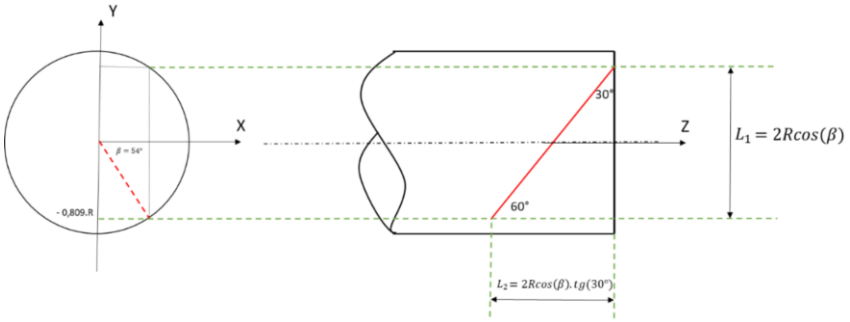

Figure 7. Position of Sensor 4.

Each sensor is only sensitive to the velocity component parallel to the directional vector of the ultrasonic beam. This way, it is necessary to determine the dot product between the velocity vector and the beam vector, to calculate the average velocity in each beam. Eq. (3) shows the calculation performed.

$$V_{i,p} = \frac{1}{L}\int_l \vec{v}(l) \cdot d\vec{s}, \tag{3}$$

where L is the acoustic path length, l is the parametrized acoustic path and s is the beam vector of sensor i in the plane p.

Additionally, the velocities measured in plane A (V_a) and in plane B (V_b), the reconstructed/composed (V_{comp}), the real axial velocity (V_z), the relation between marginal and central velocities (Velocity Ratio - V_r) and the meter error can be calculated, according to the Eqs. (4) to (8).

$$V_a = \omega_1 V_{1,a} + \omega_2 V_{2,a} + \omega_3 V_{3,a} + \omega_4 V_{4,a} \tag{4}$$

$$V_b = \omega_1 V_{1,b} + \omega_2 V_{2,b} + \omega_3 V_{3,b} + \omega_4 V_{4,b} \tag{5}$$

$$V_{comp} = \frac{V_a + V_b}{2} \tag{6}$$

$$V_r = \frac{V_{2,a} + V_{2,b} + V_{3,a} + V_{3,b}}{V_{1,a} + V_{1,b} + V_{4,a} + V_{4,b}} \tag{7}$$

$$Error\ [\%] = 100\frac{|V_z - V_{comp}|}{V_z} \tag{8}$$

3. NUMERICAL SIMULATIONS

The simulations provided the velocity and pressure fields over the entire control volume. Thus, the velocity profile in the sensors region could be raised and the theoretical velocities for each sensor calculated.

3.1 Flow results

To illustrate the results obtained with CFD, Figure 8 shows the results of pressure and velocity fields, the streamlines and the rotational velocity for water with mean inlet velocity of 8 m/s. It is possible to observe the existence of a secondary flow, characterized by two counter-rotational vortices, known as Dean vortices (Ghobadi and Muzychka, 2015).

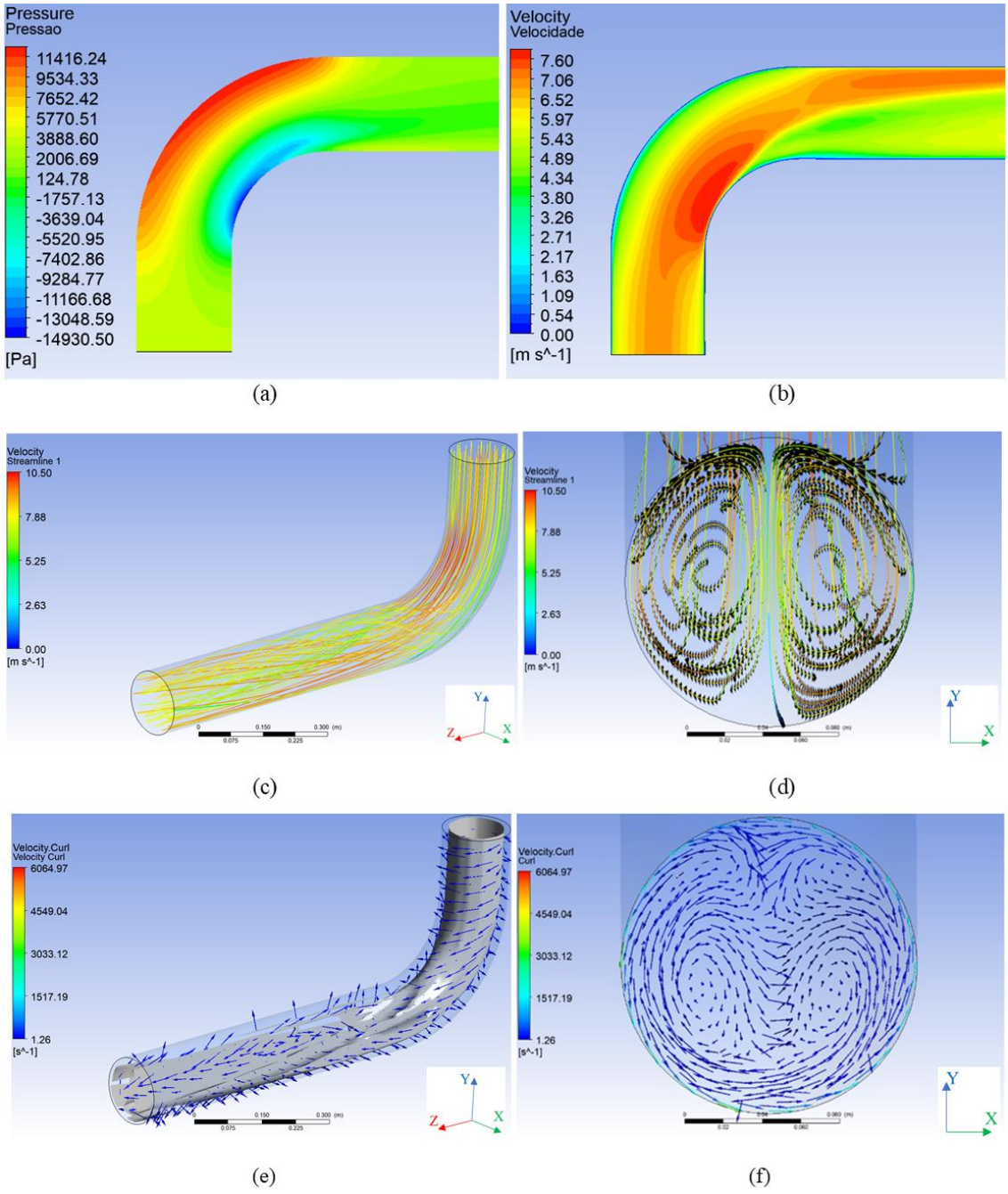

Figure 8. CFD results for water with mean inlet velocity of 8 m/s: (a) pressure and (b) velocity fields, (c,d) the streamlines and (e,f) the rotational velocity.

3.2 Flow meter data

This section presents the theoretical response for each plane and for the composition of both. Figure 9 and 10 shows the Meter Errors as function of Reynolds Number for planes A and B, respectively, and Figure 11 shows the Meter Error for the composed velocity.

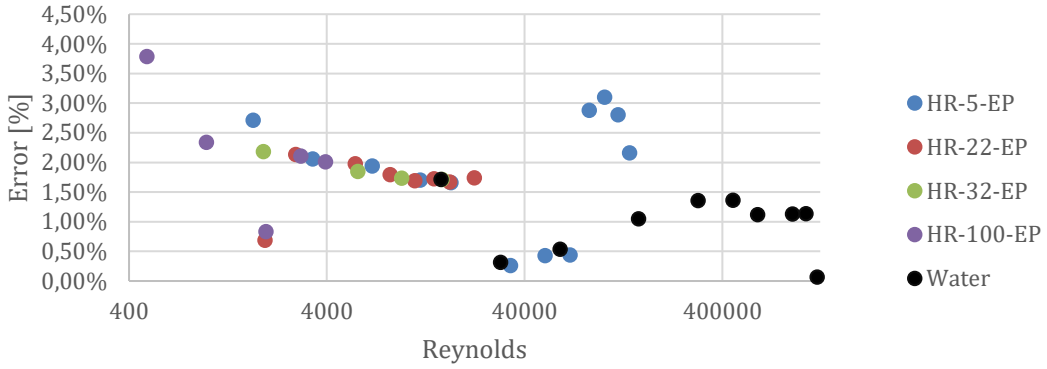

Figure 9. Error in function of Reynolds for theoretical response of the simulated meter (Plane A).

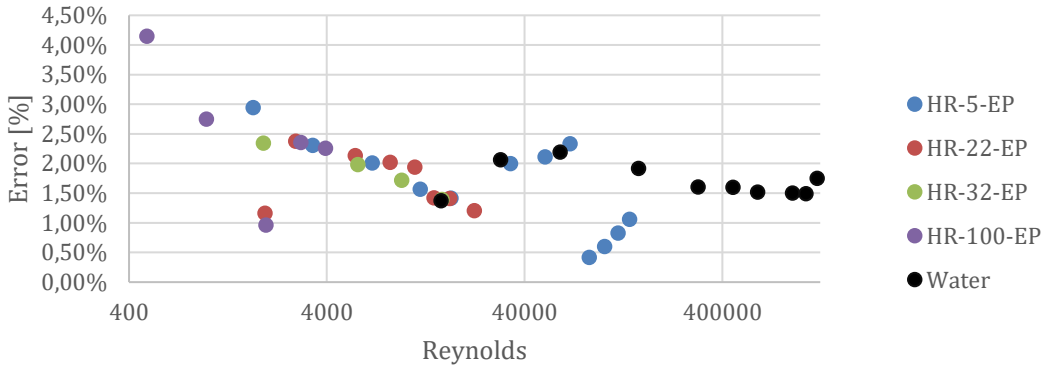

Figure 10. Error in function of Reynolds for theoretical response of the simulated meter (Plane B).

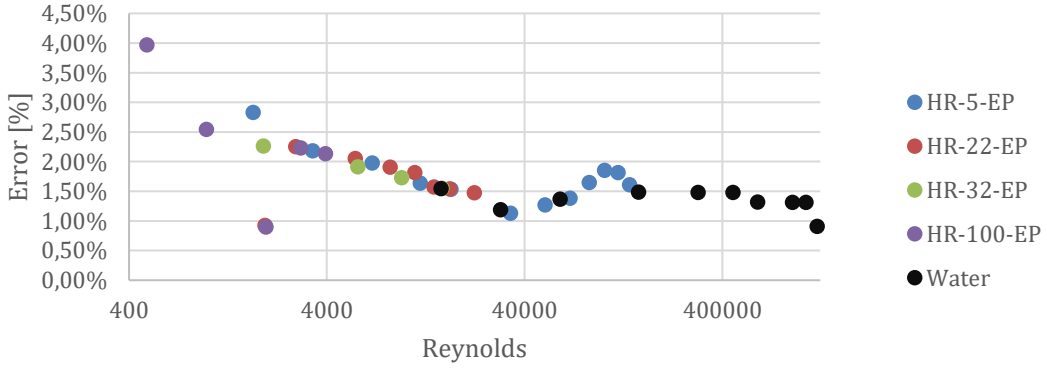

Figure 11. Error in function of Reynolds for theoretical response of the simulated meter (Composed Velocity).

The analysis of the graphics shows that the theoretical performance of multi-paths ultrasonic flowmeters is a well-defined function of the Reynolds Number, especially for the composition of Planes A and B. The use of two crossed-planes allows the reduction of influence caused by secondary flows, thus allowing a more linear and Reynolds correlated response.

4. CONCLUSIONS

The use of Computational Fluid Dynamics (CFD) allows a better understanding of the behavior of multi-path ultrasonic flowmeters installed in piping with curves upstream, where laboratory tests are typically expensive and cumbersome.

From the results obtained and the fluid dynamic concepts involved, it can be concluded that the flow profile is a function of the Reynolds number for incompressible and Newtonian flows, rest assured the condition of geometric similarity. This means that even for non-ideal installation configurations (with curves and bumps upstream of the meter), calibration against Reynolds number can be performed. It is also important to notice that the condition of geometric similarity is not exhaustive, but it was not addressed in this study.

Furthermore, the findings demonstrate that the curling influence can be significantly mitigated - or even eliminated - through the composition of velocity in two transverse planes.

5. ACKNOWLEDGEMENTS

We thank INMETRO and PETROBRAS for providing the computer and software used to run the simulations. This work was funded by PETROBRAS under grant number 4600615426.

6. REFERENCES

AGA, 2017. *AGA Report No. 9: Measurement of Natural Gas by Multipath Ultrasonic Meters*, American Gas Association, Washington-DC.

ANSYS, 2012. *FLUENT 12.0 User's Guide*, Ansys Inc, USA, https://www.afs.enea.it/project/neptunius/docs/fluent/html/ug/main_pre.htm. Accessed 20 Jun 2023.

Fox, R. W, McDonald, A. T. and Pritchard, P. J., 2011. *Introduction to fluid mechanics* (in Portuguese). LTC, Rio de Janeiro, p. 36-289.

Ghobadi, M. and Muzychka, Y. S., 2015. "A Review of Heat Transfer and Pressure Drop Correlations for Laminar Flow in Curved Circular Ducts". *Heat Transfer Engineering*, Vol. 37, n. 10, p. 815-839.

HHG, 2012. *ANSI B16.9 standard is Factory-Made Wrought Steek Butt-welding Fittings*, Hebei Haihao Group, China.

Inmetro/ANP, 2013. *Technical Regulation for Oil and Natural Gas Measurement No. 001/2013* (in Portuguese), Instituto Nacional de Metrologia, Qualidade e Tecnologia (Inmetro) and Agência Nacional do Petróleo, Gás Natural e Biocombustíveis (ANP), Rio de Janeiro, http://www.inmetro.gov.br/legislacao/rtac/pdf/RTAC001995.pdf. Accessed 21 Dec 2021.

7. RESPONSIBILITY NOTICE

The authors are the only responsible for the printed material included in this paper.